

RESEARCH ARTICLE | AUGUST 25 2003

Structural, Transport and Magnetic Properties of the Doped Magnetic Superconductor Ru-1212

A. Hassen; A. Kimmel; J. Hemberger; P. Mandal; A. Loidl

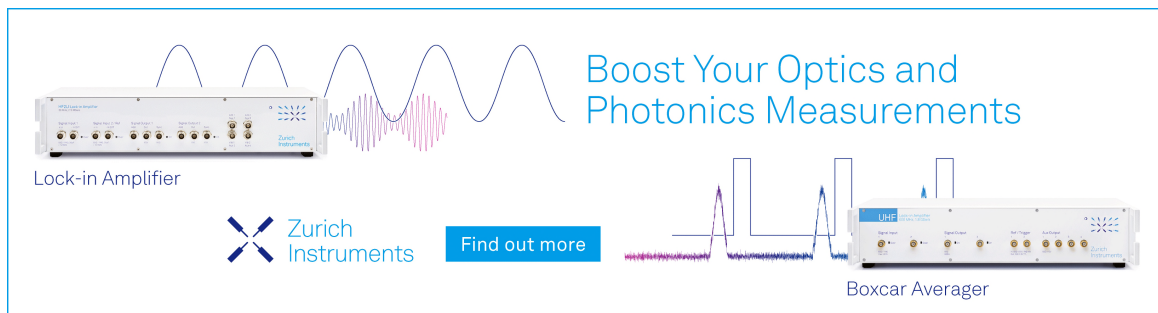


AIP Conf. Proc. 678, 333–342 (2003)


<https://doi.org/10.1063/1.1612401>



Boost Your Optics and Photonics Measurements



Lock-in Amplifier



[Find out more](#)

Boxcar Averager

Structural, Transport and Magnetic Properties of the Doped Magnetic Superconductor Ru-1212

A. Hassen*, A. Krimmel*, J. Hemberger*, P. Mandal[†] and A. Loidl*

**Institut für Physik, Elektronische Korrelationen und Magnetismus, Universität Augsburg, D-86159 Augsburg, Germany*

[†]*Saha Institute of nuclear Physics, 11AF Bidhannagar, Calcutta 700064, India*

Abstract. Single phase materials of $\text{RuSr}_2\text{Gd}_{0.5}\text{Eu}_{0.5}\text{Cu}_2\text{O}_8$ (Ru-1212Gd_{0.5}Eu_{0.5}) and $\text{Ru}(\text{Sr}_{1-x}\text{Na}_x)_2\text{GdCu}_2\text{O}_8$ ($0 \leq x \leq 0.10$) have been successfully synthesized in oxygen at 1065 °C. DC-resistivity and magnetic susceptibility measurements show a decrease of the superconducting transition temperature T_c from 46 K in the pure Gd compound to 41 K in Ru-1212Gd_{0.5}Eu_{0.5}, whereas the magnetic ordering temperature T_M does not change. The influence of the monovalent substitution Na^+ for Sr^{2+} on the properties of Ru-1212Gd is investigated and compared with previous work. Finally, the effects of Cu substituted $\text{RuSr}_2\text{Gd}(\text{Cu}_{1-x}\text{M}_x)_2\text{O}_8$ compounds, where M is Co, Ni and Ga for $0 \leq x \leq 0.03$ are reported and compared with similar doping experiments in other high- T_c superconductors.

INTRODUCTION

The antagonistic nature of superconductivity and ferromagnetism was studied theoretically by Ginzburg[1] in 1956, while experimental progress in the field began after the discovery of the so-called Chevrel phases REMo_6X_8 (RE=rare earth, X=S, Se) or in RERh_4B_4 (see for example Ref. [2]). In many of these compounds, superconductivity with a critical temperature T_c coexists with antiferromagnetic (AFM) order below the Néel temperature T_N where $T_N \ll T_c$. On the other hand, singlet superconductivity and ferromagnetism can not coexist in bulk samples with realistic physical parameters. However, under certain conditions the ferromagnetic order is transformed, in the presence of superconductivity, into a spiral or domain-like structure depending on the type and strength of magnetic anisotropy in the system [3]. The internal field of a ferromagnetically ordered state leads to a Zeeman splitting of the Fermi surface that excludes electron pairing of opposite spin and momentum. Allowing for finite angular momentum of electron pairs led to the theory of Fulde-Ferrel-Larkin-Ovchinnikov (FFLO) superconductivity [4], where a suitable spatial modulation of the superconducting or ferromagnetic order parameter (or both) leads to their mutual coexistence.

Recently, a new class of magnetic superconductors among the layered perovskite ruthenocuprates $\text{RuSr}_2\text{RECu}_2\text{O}_8$ (Ru-1212RE, RE = Gd, Eu, Y and Sm) has been synthesized [5]. In particular, the Ru-1212Gd system has attracted great interest since it exhibits a ferromagnetic transition at $T_M \approx 135$ K and bulk superconductivity below $T_c \approx 46$ K, depending on the sample preparation conditions [6, 7, 8]. For the isostructural Ru-1212Eu compound, these transitions are shifted to 133 K and 32 K, respectively.

The tetragonal crystal structure of both Gd- and Eu-based Ru-1212 is very similar to

the prototype high- T_c cuprate superconductors REBa₂Cu₃O_{7- δ} (RE-123) [6, 9, 10]. The structure of Ru-1212RE contains CuO₂ bilayers carrying superconductivity and RuO₂ monolayers substituting the CuO chains of the RE-123 compounds.

Neutron powder diffraction measurements [10, 11] revealed a *G*-type AFM structure of the Ru sublattice with an ordered magnetic moment of the order of $1\mu_B$. The ferromagnetic ordering observed in magnetic experiments can be accounted for by a canting of the Ru moments. However, the origin of the FM component is still unclear. Both neutron powder diffraction studies lead to upper limits of any net FM component of $0.3\mu_B$ [11] or $0.1\mu_B$ [10], respectively. The mixed valent state of the Ru ions, as evidenced by XANES [12] and NMR [13] spectroscopy enables a double exchange interaction between different Ru ions and the proportion of Ru⁴⁺/Ru⁵⁺ ions may change with cation substitution in Ru-1212RE. Therefore, the hole concentration in the superconducting CuO₂ planes may be changed in a controlled way by doping [12]. In case of the cuprate superconductors for example, hole carriers can be induced either by cation substitution (as in La_{2x-1}Sr_xCuO₄) or by oxygen intercalation (as in YBa₂Cu₃O_{7- δ}) or by a combination of them. Unlike the RE-123 compounds, the oxygen content of Ru-1212RE can virtually not be changed. Thermogravimetric experiments [14, 15], as well as the thermoelectric power (TEP) [16] indicate that the oxygen content is always very close to 8. In order to change the hole carrier concentration in Ru-1212RE, one therefore has to rely on cation substitution [17, 18]. The effect of substituting cations on the electrical and magnetic properties of Ru-1212Gd was reported by different groups [12, 18, 19, 20, 21, 22]. It is generally observed that both magnetism and superconductivity depend on the type of cation and the substitutional site. It was noticed that Ti and Rh doping reduced the magnetic ordering temperatures [22] while Nb and V enhanced it [18, 20]. T_c decreases for all cations investigated so far, except in case of Ru_{1-x}Sr₂GdCu_{2+x}O₈, where it reaches 70 K for $x = 0.7$ [19].

In this work, we first complete the comparison between pure Gd and Eu-based compounds by investigating Ru-1212Gd_{0.5}Eu_{0.5}. Then we compare previous results of doped Ru-1212Gd compounds [21, 22] with a new type of substitution Ru(Sr_{1-x}Na_x)₂GdCu₂O₈ for $0 \leq x \leq 0.10$. Finally, the T_c -suppression by copper substituting cations RuSr₂Gd(Cu_{1-x}M_x)₂O₈, (M = Co, Ni and Ga) for $0 \leq x \leq 0.03$ is studied and compared with Zn-doping in Ru-1212Gd [23] and other high- T_c superconductors.

EXPERIMENTAL DETAILS

Polycrystalline samples have been synthesized by a solid-state reaction method [23] using high purity RuO₂, SrCO₃, Gd₂O₃, CuO, NiO, Ga₂O₃, CoO and Na₂O powders. At the final stage, the samples were annealed for 6 days at 1065 °C in flowing oxygen followed by slow cooling down to room temperature. Powder x-ray diffraction (PXD) data at room temperature were collected on a Stoe x-ray diffractometer using the Cu-K α radiation ($\lambda = 1.5406 \text{ \AA}$) in the range of $20^\circ \leq 2\theta \leq 80^\circ$ at an increment of 0.02° . The data were analyzed by standard Rietveld refinement. Magnetic measurements were performed employing a SQUID magnetometer (Quantum Designs, MPMS). The resistivity was measured by a conventional four-probe technique.

RESULTS AND ANALYSIS

Crystal Structure

Based on Rietveld analyses of XRD patterns, all samples are found to be single phase except for the pure Eu-based compounds which exhibit an additional very weak intensity close to $2\theta \approx 31.5^\circ$. This spurious reflection is attributed to residues of SrRuO_3 or Gd_2CuO_4 [24] and its occurrence is well-known for the Ru-1212RE system. The tetragonal lattices of the pure Gd- and Eu-based samples are in good agreement with previous reports [5, 6, 18, 25]. The lattice parameters of $\text{Ru-1212Gd}_{0.5}\text{Eu}_{0.5}$ are $a = b = 3.842 \text{ \AA}$ and $c = 11.573 \text{ \AA}$ which are close to those of the pure compounds. Moreover, all diffraction patterns of the $x = 0, 0.03$ and 0.10 Na-doped compounds could be successfully indexed on the basis of the usual tetragonal unit cell with space group $P4/mmm$, as shown in Fig. 1. The crystallographic structures remain almost unchanged within the present range of doping.

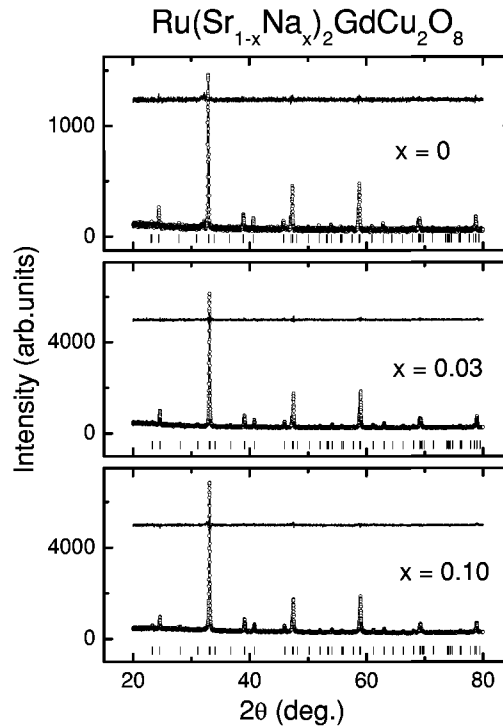


FIGURE 1. Room temperature x-ray diffraction patterns of $\text{Ru}(\text{Sr}_{1-x}\text{Na}_x)_2\text{GdCu}_2\text{O}_8$ for $x = 0, 0.03$ and 0.10 . The vertical bars denote the peak positions as indexed by space group $P4/mmm$. The intensities as calculated on the basis of the Rietveld refinement are indicated as solid lines. The difference between observed and calculated intensities are shown at the top of each pattern.

Magnetic Properties

Fig. 2 shows the temperature dependence on dc magnetic susceptibility $\chi(T) = M/H$ at an external field of $H = 1$ kOe. As expected, $\chi(T)$ of Ru-1212Gd_{0.5}Eu_{0.5} is located between the pure Gd- and Eu-based compounds. This implies that only the Gd moments contribute to the total magnetization of the doped sample whereas Eu is nonmagnetic. There is no change in T_M for the mixed compound since the RuO₂ layers are responsible for the magnetic ordering in Ru-1212RE. Similarly, Bernhard et al. [26] reported that the ferromagnetic transition is not significantly affected by the partial substitution of non-magnetic Y³⁺ for the magnetic Gd³⁺ ions. The inverse magnetic susceptibility, $\chi^{-1}(T)$ of both Ru-1212Gd and Ru-1212Gd_{0.5}Eu_{0.5} were fitted using two independent Curie-Weiss functions, where the parameters of Gd were kept fixed at $\theta_{Gd} = -4$ K and $\mu_{eff} = 7.94 \mu_B$ [21]. The $\chi^{-1}(T)$ data of Ru-1212Eu were fitted at $T \geq 200$ K by using a susceptibility $\chi^{-1}(T) = (1/(T + \theta) + \chi_0)^{-1}$, where χ_0 is the temperature independent part. Its value of $\chi_0 = 3.34 \times 10^{-3}$ emu/mol is in agreement with earlier reports [27]. It is noticed that the value of the magnetic parameters significantly depend on the rare earth element.

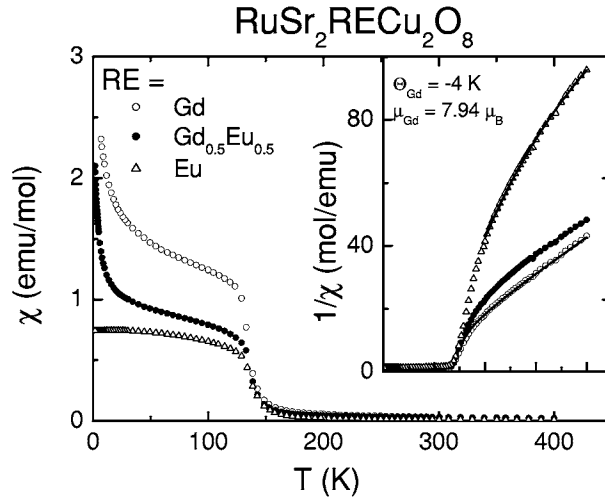


FIGURE 2. The temperature dependence of dc susceptibilities $\chi_{dc}(T)$ at 1 kOe for RuSr₂Gd_{0.5}Eu_{0.5}Cu₂O₈, as well as for the pure Gd- and Eu-based compounds. The inset shows the corresponding inverse susceptibilities $\chi^{-1}(T)$ including the Curie-Weiss fitting functions (solid lines)

The substitution of monovalent Na⁺ for Sr²⁺ in Ru-1212Gd is now compared with La-doping [21]. Fig. 3 shows $\chi(T)$ (upper frame) for $x = 0, 0.03$ and 0.10 Na-doping at an external field 1 kOe. Similar to La-doping, the magnetic ordering temperature T_M is enhanced while at low temperatures the magnetic moments are decreased with increasing Na concentration x due to an increase of the canting angle of the Ru moments. The inset of the figure shows FC/ZFC curves of the sample $x = 0.03$. A splitting at the magnetic ordering temperature is observed like for the pure and La-doped Ru-1212Gd compounds. There is no clear evidence about the absence of a Meissner effect down to

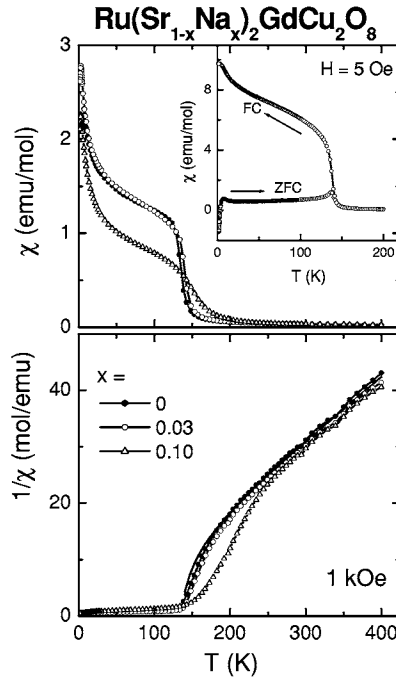


FIGURE 3. Temperature dependence of the dc susceptibility (upper frame) of $\text{Ru}(\text{Sr}_{1-x}\text{Na}_x)_2\text{GdCu}_2\text{O}_8$ for $x = 0, 0.03$ and 0.10 at an external field of 1 kOe and the corresponding inverse susceptibility (lower frame). The inset shows FC/ZFC measurements for $x = 0.03 \text{ Na}$ at $H = 5 \text{ Oe}$.

2 K . The sample $x = 0.03$ clearly is a superconductor while for the same La concentration superconductivity is already completely suppressed [21]. The lower frame of the figure shows $\chi^{-1}(T)$ of some Na-doped samples and the data can be fitted as for pure and La-doped Ru-1212Gd. It is evident that any change in the SrO layers caused by either Na or La substitution, respectively enhances the magnetic ordering temperature and destroys superconductivity in Ru-1212Gd. However, the physical origin must be different for the two doping series since the substitution of Na^+ for Sr^{2+} corresponds to hole doping, whereas the substitution of La^{3+} for Sr^{2+} corresponds to electron doping.

The dependence of the real part of the ac susceptibility χ' on magnetic field at constant temperatures for $x = 0.03 \text{ Na}$ is shown in Fig. 4. As in case of the pure and La-doped Ru-1212Gd compounds, the data were taken after zero-field cooling at 1 Hz with an ac field of 1 Oe from above and below T_M . Maxima in the field dependence of χ' can be detected and signal a metamagnetic transition. The corresponding phase diagram, where the solid points separate a ferromagnetic (FM) phase at high fields from a canted antiferromagnetic (CA) phase at low fields is illustrated in the inset of Fig. 4. The $H - T$ phase diagram of the Na-doped compounds is similar to the La-doped one, where the ferromagnetic phase transition can be induced by fields smaller than 1 kOe [21].

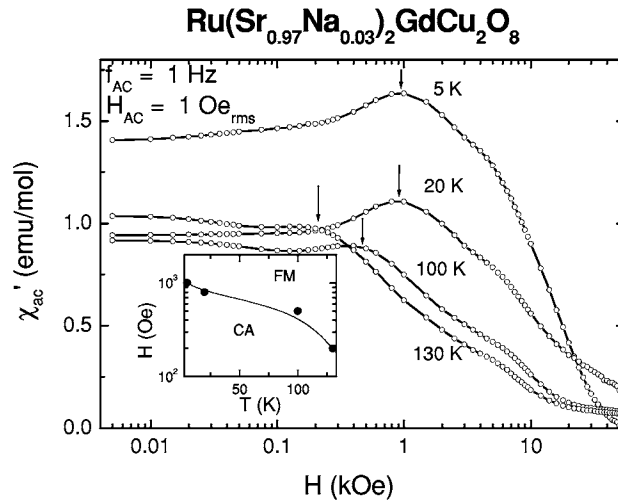


FIGURE 4. Field dependence of the real part of the ac-susceptibility for the $x = 0.03$ Na doped sample at different temperatures below T_M . The arrows indicate a characteristic temperature where a metamagnetic transition occurs. The inset shows a schematic (H, T) phase diagram separating a canted antiferromagnetic (CA) from a purely ferromagnetic (FM) phase.

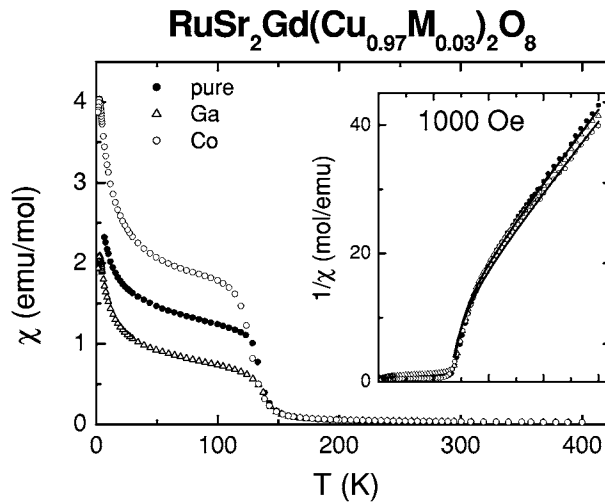


FIGURE 5. Temperature dependence of the dc-susceptibilities $\chi_{dc}(T)$ for $x = 0.03$ Ga and Co, including the pure Gd compound for comparison, as measured on cooling at $H = 1$ kOe. The inset shows the corresponding inverse susceptibility $1/\chi_{dc}(T)$.

For $\text{RuSr}_2\text{Gd}(\text{Cu}_{1-x}\text{M}_x)_2\text{O}_8$ ($M = \text{Ga}, \text{Co}, \text{Ni}$) the dc magnetic susceptibility was also measured at an external field 1 kOe. The pure sample is included for comparison. Fig. 5 shows $\chi_{dc}(T)$ for $x = 0.03$ Ga and Co. As can be observed from the figure, the

magnetic susceptibility of the Ga-doped compound lies well below that of the pure and Co substituted compound as Ga is nonmagnetic whereas Co has a large magnetic moment. The magnetic ordering temperature T_M is not changed as it reflects the fact that the ferromagnetism in Ru-1212RE originates from the RuO₂ layers. The inset shows $\chi^{-1}(T)$ for the same concentration of Co and Ga. As in the pure compounds, the data were fitted in terms of two independent Curie-Weiss functions. As it is expected, the effective magnetic moment of the Ru sublattice for the $x = 0.03$ Co-doped sample, ($\mu_{eff} = 3.37 \mu_B$) is larger than for the 3% Ga-doped sample ($\mu_{eff} = 2.96 \mu_B$) due to the magnetic contribution of Co to the Ru moments. This is in contrast to other HTSCs, where the magnetism is enhanced for both, magnetic and non-magnetic copper substituted cations [28].

dc-Resistivity

The zero-field resistivity ρ of bulk Ru-1212Gd_{0.5}Eu_{0.5} exhibits a maximum around $T_c = 41$ K and drops to zero slightly above 19 K. For pure Ru-1212Eu/Gd, ρ shows maxima around 34 and 51 K, respectively [29, 21]. It is clear that any small structural changes affect the superconducting and magnetic properties. The decrease of T_c with substitution of Gd by Eu can also be attributed to the change of the bond angle ϕ (Ru-O-Cu) which affects the transfer of charge carriers between RuO₂ and CuO₂ layers. From the Rietveld analysis, it was found that the value of ϕ (Ru-O-Cu) for Ru-1212Gd_{0.5}Eu_{0.5} is slightly smaller than that of pure Ru-1212Gd compounds.

The dc resistivity of Na-doped samples was measured at zero external magnetic field, as shown in Fig. 7. The resistivity increases with increasing Na concentration but the sample with $x = 0.03$ is still superconducting with an onset temperature of $T_c = 45$ K.

The observed decrease of T_c by substituting Sr partially by Na was not expected. Since Na is a monovalent ion and Sr is divalent, Na substitution can be considered as a hole doping leading to an increase of the charge carrier concentration in the system. Therefore, other factors must prevent an increase of T_c with increasing Na concentration such as trapping of the charge carriers. Another reason of a decreasing T_c induced by La and Na doping may be due to the closeness of the SrO layers to the superconducting CuO₂ layers so that even minor changes on a local scale within the SrO₂ layers may have a strong effect. As shown in the inset of the Fig. 7, the Na-doped sample for $x = 0.10$ has a very similar semiconducting behavior in the whole temperature range as the 10% La-doped compound.

As reported earlier [31, 32, 33, 34, 35], impurities in the copper planes rapidly destroy superconductivity due to pair breaking. The concentration range of impurities and the rate of the T_c suppression depend on the type of the substituting cations, as well as on the HTSCs material itself. The resistivity of RuSr₂Gd(Cu_{1-x}M_x)₂O₈ ($M = \text{Ga, Co and Ni}$) was measured at zero external field. Fig. 8 shows the temperature dependence of the resistivity of Ni-doped samples as a typical example of copper substitution. It is noticed that the resistivity increases with increasing Ni and superconductivity is fully suppressed at $x = 0.03$. The upper inset in this figure shows the resistivity for $x = 0.03$ Ni which is non-superconducting and the resistivity increases for decreasing T in the

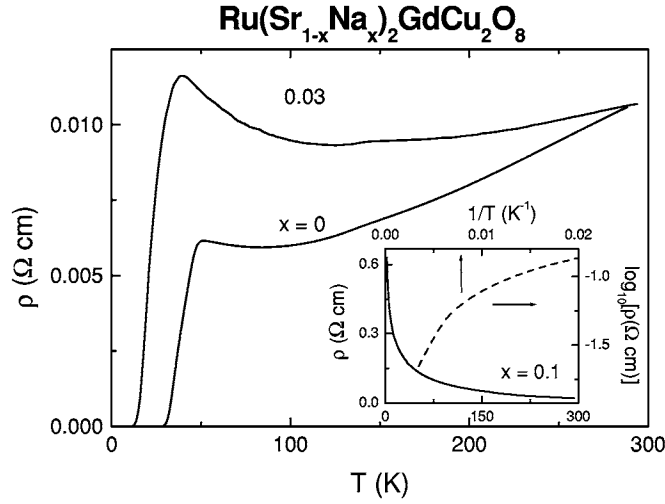


FIGURE 6. dc resistivity vs. temperature of $\text{Ru}(\text{Sr}_{1-x}\text{Na}_x)_2\text{GdCu}_2\text{O}_8$ for $x = 0, 0.03$ and 0.1 . The resistivity for $x = 0.10$ is shown in the inset: ρ vs. T (solid line, left and lower scale) and $\log \rho$ vs. T^{-1} (dashed line, right and upper scale).

whole temperature range. Similarly, Bernhard et al.[36] reported that T_c in Ru-1212Gd was completely destroyed for 0.03 Zn-doping. The lower inset summarizes the change of T_c with different substituted cations. Evidently, Co suppresses the superconductivity faster than Ga and Ni. This may be attributed to the large magnetic moment of Co, leading correspondingly to a strong pair breaking effect. Compared to other HTSCs, Xiao et al.[37] reported on the substitution of 3d elements at the Cu site in $\text{YBa}_2\text{Cu}_3\text{O}_{7-\delta}$ (YBCO). They observed that T_c is reduced to zero beyond a critical concentration which varies from element to element. For example, non-magnetic Zn ions have a stronger influence on T_c than magnetic Co ions. Moreover, Tarascon et al. [28] show that superconductivity in YBCO is preserved for a large doping range up to $x = 0.3$ for Fe or Co and up to $x = 0.5$ for Ni. On the other hand, superconductivity in Ru-1212 is completely suppressed at very low concentrations of copper substitution ($x \leq 0.03$). Similarly, 2.5% Zn impurities are sufficient to suppress the superconductivity in $\text{La}_{1.85}\text{Sr}_{0.15}\text{Cu}_{1-x}\text{Zn}_x\text{O}_4$ (Ref.[34]).

CONCLUSIONS

We have successfully synthesized two novel substitutional series $\text{Ru}(\text{Sr}_{1-x}\text{Na}_x)_2\text{GdCu}_2\text{O}_8$ ($0 \leq x \leq 0.10$) and $\text{RuSr}_2\text{Gd}(\text{Cu}_{1-x}\text{M}_x)_2\text{O}_8$ ($M = \text{Co}, \text{Ni}, \text{Ga}, 0 \leq x \leq 0.03$), as well as the mixed compound $\text{RuSr}_2\text{Gd}_{0.5}\text{Eu}_{0.5}\text{Cu}_2\text{O}_8$. Powder x-ray diffraction revealed single phase materials and only minor crystallographic changes as compared to pure Ru-1212Gd for all investigated compounds. Changes of the physical behavior of Ru-1212Gd are known to be sensitive to both, substituent and substitutional site. Na

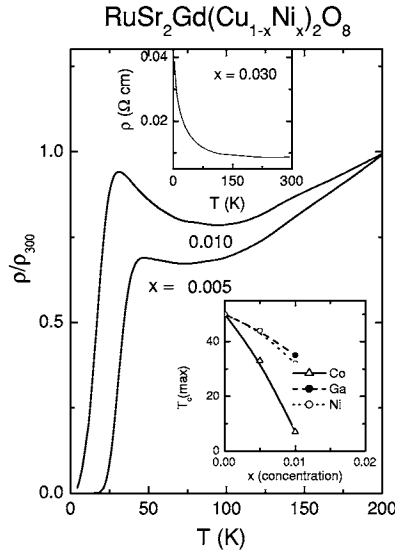


FIGURE 7. Normalized electrical resistivity (ρ/ρ_{300}) vs. temperature for Ni-doped Ru-1212. The upper inset shows the resistivity for $x = 0.03$ while the lower inset shows the change of T_c for different copper substituting elements.

doping has been chosen in order to study the effect of hole doping. Moreover, exchange of Cu ions for Co, Ni or Ga respectively probes the effect of impurities within the superconducting CuO-planes. The magnetic and superconducting properties of doped Ru-1212Gd were studied by means of resistivity and magnetic measurements.

Because the ferromagnetism in the rutheno-cuprate system is due to the RuO_2 layers (apart from the very low temperature region), there is no change of T_M for an equal mixture of Eu and Gd rare earth ions ($\text{Ru-1212Gd}_{0.5}\text{Eu}_{0.5}$). Similar to the effect of La-doping, T_M is enhanced and T_c suppressed by Na-doping but at a different rate. It can be considered that monovalent Na-doping increases the hole concentration in the system because it substitutes a divalent cation (Sr^{2+}). The decrease of T_c with increasing Na content may therefore be attributed to other effects like trapping of charge carriers. Superconductivity is suppressed rapidly by copper substitution due to pair-breaking as generally observed in HTSCs. The effect of Co substitution is stronger than the effect of magnetic Ni or non-magnetic Ga impurities because of its large magnetic moment. Compared with 3d-element doped YBCO, superconductivity is destroyed very rapidly in Ru-1212RE and implies that the major contribution to superconductivity originates from the copper-oxide planes. Moreover, the decrease of the magnetic moment at low temperatures for Ga substitution and its increase for Co or Ni suggests that there is a contribution of the CuO-planes to the total magnetic moment of the system.

ACKNOWLEDGMENTS

This work was partly supported by Bundesministerium für Bildung und Forschung (BMBF) via VDI/EKM 13 N 6917 and by the Deutsche Forschungsgemeinschaft via SFB484, Augsburg.

REFERENCES

1. V. L. Ginzburg, *Sov. Phys. JETP*, **4**, 153 (1957).
2. "Superconductivity in ternary compounds", edited by M. B. Maple and Ø. Fisher, (Berlin, **II**, 1982).
3. L. N. Bulaevskii et al., *Adv. Phys.* **34**, 176 (1985).
4. P. Fulde and R. A. Ferrell, *Phys. Rev.* **135**, A550 (1964); A. I. Larkin and Yu N. Ovchinnikov, *Zh. Eksp. teor. Fiz* **47**, 1136 (1964).
5. L. Bauerfeind, W. Widder and H. F. Braun, *Physica C* **254**, 151 (1995); *J. Low Temp. Phys.* **105**, 1605 (1996).
6. I. Felner et al., *Physica C* **311**, 163 (1999).
7. C. Artini et al., *Physica C* in press.
8. T. Papageorgiou et al., *Physica C* in press.
9. A. C. McLaughlin et al., *Phys. Rev. B* **60**, 7512 (1999).
10. O. Chmaissem et al., *Phys. Rev. B* **61**, 6401 (2000).
11. J. W. Lynn et al., *Phys. Rev. B* **61**, 14964 (2000).
12. R. S. Liu et al., *Phys. Rev. B* **63**, 212507 (2001).
13. K. Kumagai, S. Takada and Y. Furukawa, *Phys. Rev. B* **63**, 180509 (2001).
14. K. Otzsch et al., *J. Low. Temp. Phys.* **117**, 855 (1999).
15. P. W. Klamut et al., *Physica C* **341-348**, 455 (2000).
16. B. Lorenz et al., *Physica C* **363**, 251 (2001).
17. J. Tallon et al., *IEEE. Trans. App. Super.* **9**, 1696 (1999).
18. A. C. McLaughlin and J.P. Attfield, *Phys. Rev. B* **60**, 14605 (1999); A.C. McLaughlin et al., *J. Mater. Chem.* **11**, 173 (2001).
19. P. W. Klamut et al., *Phys. Rev. B* **63**, 224512 (2001); P. W. Klamut et al., *Physica C* **350**, 24 (2001).
20. J. T. Rijnssenbeek et al., *Physica C* **341-348**, 481 (2000); S. Malo et al., *J. Inorg. Mater.* **2**, 601 (2000).
21. P. Mandal et al., *Phys. Rev. B* **64**, 144506 (2002).
22. A. Hassen et al., *Phys. Rev. B*, submitted.
23. J. L. Tallon et al., *Phys. Rev. B* **61**, 4671 (2000).
24. M. Hrovat et al., *J. Mater. Sci. Lett.*, **19**, 919 (2000); M. Hrovat et al., *J. Mater. Sci. Lett.*, **19**, 1423 (2000).
25. D. P. Hai et al., *Physica C* **357-360**, 406 (2001).
26. C. Benhard et al., *Phys. Rev. B* **59**, 14099 (1999).
27. G. V. M. Williams and S. Krämer, *Phys. Rev. B* **62**, 4132 (2000).
28. J. M. Tarascon et al., *Phys. Rev. B* **36**, 8393 (1987); J. M. Tarascon et al., *Phys. Rev. B* **37**, 7458 (1988).
29. R. L. Meng et al., *Physica C* **353**, 195 (2001).
30. B. Lorenz et al., *Phys. Rev. B* **65**, 174503 (2002); B. Lorenz et al., *cond-mat/Nr.*, (unpublished).
31. G. V. M. Williams and J. L. Tallon, *Phys. Rev. B* **57**, 10984 (1998).
32. J. L. Tallon and G. V. M. Williams, *Phys. Rev. B* **61**, 982 (2000).
33. Ratan Lal et al., *Phys. Rev. B* **49**, 6382 (1994).
34. K. Westerholt et al., *Phys. Rev. B* **39**, 11 680 (1989).
35. G. V. M. Williams et al., *Phys. Rev. B* **54**, 9532 (1996).
36. C. Bernhard et al., *Phys. Rev. B* **61**, 14960 (2000).
37. G. Xiao et al., *Phys. Rev. B* **35**, 8782 (1987).